IOP Publishing Journal of Optics
J. Opt. **27** (2025) 065502 (8pp) https://doi.org/10.1088/2040-8986/ade1ea

Switching of noise-like pulse and dissipative pulse state in a mode-locked dual-wavelength Yb-doped picosecond fiber laser via nonlinear polarization rotation

Fei He[1], Xincheng Huang[1], Xinyang Su[1,*], Tao Zhang[1], Yifei Chen[1], Zhaoyang Tian[1], Bohan Li[1], Yu Li[1], Jianwei Li[2], Hanbin Wang[1,3,*] and Sergey Kobtsev[4]

[1] School of Physical Science and Engineering, Beijing Jiaotong University, Beijing 100044, People's Republic of China
[2] Zhejiang Provincial Innovation Center of Laser Intelligent Equipment Technology, Wenzhou, Zhejiang 325200, People's Republic of China
[3] Weihai Institute of Beijing Jiaotong University, Weihai 264401, People's Republic of China
[4] Division of Laser Physics and Innovative Technologies, Novosibirsk State University, Novosibirsk 630090, Russia

E-mail: xysu@bjtu.edu.cn and hbwang1@bjtu.edu.cn

Received 27 April 2025, revised 27 May 2025
Accepted for publication 6 June 2025
Published 17 June 2025

Abstract

Based on the principle of nonlinear polarization rotation (NPR), we propose and experimentally demonstrate a mode-locked dual-wavelength Yb-doped fiber laser. Flexible switching between the noise-like pulse (NLP) and dissipative pulse regimes can be realized through the tuning of a single polarization controller. Experimental results validate the feasibility of the proposed technique, with stable dual-wavelength operation maintained throughout both pulse states due to Raman scattering-induced Stokes shift within the fiber. Under NLP operation, the laser exhibits a maximum output power of 140.90 mW and a slope efficiency of 12.10%. The pedestal pulse widths for the two emission wavebands (1055 nm and 1104 nm) are measured as approximately 28.65 ps and 97.25 ps, respectively, while the corresponding spike pulse widths are as narrow as 0.68 ps and 0.51 ps. In the dissipative pulse state, the maximum output power further increases to 156.40 mW with a slope efficiency of 14.60%, and a pulse width of 23.61 ps is measured at 1044 nm.

Keywords: dual-wavelength, noise-like pulses, mode-locking, fiber lasers

1. Introduction

Ultrashort pulsed lasers are characterized by short pulse duration, high peak power, and high repetition rate. They play an important role in many fields such as precision cutting and welding, material processing, medical treatment, optical communication, etc [1]. Yb-doped mode-locked fiber lasers have unique properties and application scenarios. Compared with other rare earth ions doped fiber lasers, the conversion efficiency is higher and the gain bandwidth is also wider, which enables the laser output within a wider spectral range (up to a few hundred nanometers). Therefore, Yb-doped fiber (YDF) lasers have received widespread

* Authors to whom any correspondence should be addressed.

attention and is one of the focuses of researchers. There are several different passive mode-locked methods, such as saturable absorbers (SAs) [2], nonlinear optical loop mirror, nonlinear amplifying loop mirror [3], and NPR. Among them, NPR is one of the most low-cost methods, since sometimes only one polarization controller (PC) and one isolator are used in a ring cavity to realize mode-locking, which makes it a simple and cost-effective route for mode-locking. Also, this method usually has one more tuning degree of freedom compared with others, that is the polarization state in the fiber. NPR mode-locked fiber lasers offers advantages such as narrow output pulses, wide spectral coverage, and the capacity to withstand high pulse energy [4]. There have been many reported works about NPR mode-locked YDF lasers. Gupta *et al* reported for the first time the generation of stable chair-like pulses in an all-normal dispersion Yb-doped mode-locked fiber laser based on NPR and studied their formation mechanism and amplification characteristics [5]. Dong *et al* first experimentally demonstrated the generation of noise-like square pulses in a linear-cavity mode-locked YDF laser based on NPR [6]. Geng *et al* demonstrated a switchable multi-wavelength passively mode-locked fiber laser in the 1 μm regime by utilizing the NPR mechanism for generating mode-locked pulses and the single-mode-multimode-single-mode structure as the spectral filter [7]. Pu *et al* demonstrated a hybrid mode-locked (hybrid-ML) YDF laser combining NPR and a Lyot filter, enhancing stability against environmental perturbations while maintaining mode-locking under significant fiber loop radius changes (7.5–1.5 cm) [8]. Wang *et al* constructed an Yb-doped mode-locked fiber laser via NPR. By adjusting two intracavity PCs, they observed five nonlinear regimes, including soliton explosion and pulsation, and used DFT to analyze their real-time spectra evolution [9]. Pu *et al* proposed a method for NPR mode-locking and wavelength-tuning of a fiber laser based on optical speckle. They utilized the Tamura texture feature theory to analyze speckle characteristics for mode-locking assistance and a convolutional neural network to identify wavelengths [10]. Ahmad *et al* developed a mode-locked fiber laser that adopting the hybrid passive mode-locking technology and is equipped with a novel copper oxide-doped zinc oxide SA (CuO–ZnO SA). The hybrid-ML fiber laser integrated the NPR technology with the CuO–ZnO–SA, producing remarkable characteristics with a central wavelength of 1045 nm, a 3-dB bandwidth spanning 18.26 nm, an ultra-short pulse width of 98 fs, a repetition rate of 1.96 MHz, and an impressive signal-to-noise ratio (SNR) of 51 dB [11]. Duan *et al* proposed a novel Yb-doped ultrafast fiber laser based on nonlinear multimode interference-NPR hybrid-ML mechanism. Stable single-pulse mode-locked state was achieved in the linear cavity, with a repetition rate of 12.80 MHz [12]. Except the output of single-wavelength pulses, the dual-wavelength pulses are also required for some nonlinear experiments, in particular, difference frequency mixing can generate long-wavelength radiation [13, 14]. Li *et al* observed the evolution of the soliton bunch to dissipative soliton resonance (DSR) pulses in an erbium-doped mode-locked fiber laser by introducing NPR and a multimode fiber PC (MMF-PC). The experimental results show that the MMF-PC are crucial for the evolution of soliton pairs to DSR pulses as well as the generation of soliton pairs, and that dual-wavelength mode-locking can be achieved by adjusting the PC to control the birefringence and loss in the resonator. Multiple groups of dual-wavelength outputs are achieved, including 1555.64 nm and 1560.54 nm (synchronous mode-locking), 1553.97 nm and 1561.73 nm (asynchronous mode-locking), and 1555.63 nm and 1560.82 nm (stable asynchronous mode-locking) [15]. Li *et al* employed a SA composed of two cascaded single mode fiber-graded-index multimode fiber-single mode fiber (SMF-GIMF-SMF) structures to study the generation and characteristics of noise-like pulses (NLPs), DSR pulses, and dual-wavelength (1565.95 nm and 1561.09 nm) pulses in the anomalous dispersion region by adjusting the PC and pump power [16]. Thulasi *et al* proposed an all-fiber Yb-doped mode-locked laser using a single-mode-few-mode-single-mode fiber (SMF-FMF-SMF) structure as a SA. By adjusting the intracavity birefringence, a wide wavelength tuning range of 47 nm was achieved with the central wavelength varying from 1028.88 nm to 1076.18 nm. Meanwhile, dual-wavelength switching from 1033.32/1058.2 nm to 1049.7/1075.7 nm was realized, with pulse widths compressed to the 300 fs order, demonstrating the potential of few-mode fibers in wide-tunable and dual-wavelength mode-locked fiber lasers [17]. Tang *et al* used a semiconductor SA mirror (SESAM) to achieve dual-wavelength harmonic mode-locked DSR in an all-normal dispersion YDF laser. In the fundamental frequency (3.5 MHz) mode-locking state, the pulse width and energy increased with pump power while the peak power remains constant. By adjusting the position of the SESAM, harmonic mode-locking states from the 2nd to 9th order were obtained, with the repetition rate increased to 31.5 MHz. The dual wavelengths were centered at 1072.5 nm and 1079.5 nm, respectively [18]. However, it is found that a large separation of the peak wavelength is usually difficult due to the inherent transmission setting of the fiber itself.

In this study, we demonstrate a mode-locked dual-wavelength ytterbium-doped fiber laser system employing NPR for pulse generation. Through optimization of the cavity design, particularly the length of the fiber, we achieve Raman scattering that enables simultaneous mode-locking at two distinct wavelengths. The system generates stable pulse trains with a remarkable spectral separation of 49 nm between the fundamental wavelength at 1055 nm and the Stokes-shifted wavelength at 1104 nm, representing one of the spectral separations reported for NPR-based dual-wavelength fiber lasers, which can be used for further nonlinear optics study.

2. Experiments setup

A ring cavity YDF laser based on NPR mode-locking was constructed, and the structure of the entire experimental setup is shown in figure 1.

The resonant cavity of the laser in the figure contains YDF, polarization dependent isolator (PD-ISO), output coupler, PC, wavelength-division multiplexer, and the devices are coupled

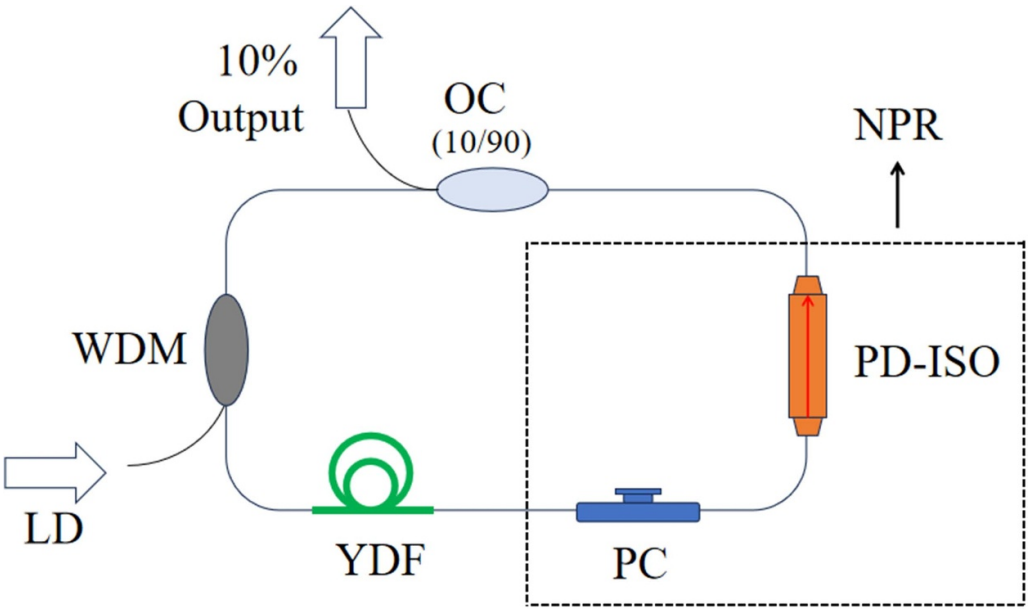

Figure 1. Diagram of the experimental setup of a ring cavity Yb-doped fiber (YDF) laser based on NPR mode-locking.

by a SMF, and the entire length of the resonant cavity is about 7.5 m. Among them, the pump source is a laser diode with a wavelength of 976 nm, and the maximum output power is 1191 mW. The length of YDF is 1.5 m, of which the model is SM-YDF-5/130-VII, and the coupling ratio of the OC is 10/90. Finally, the model of all the passive fiber is SM-GDF-5/130. The single PC used in this experiment is placed in front of PD-ISO, which is convenient for centralized adjustment of the initial polarization state of NPR. A single PC can not only reduce losses but also reduce the complexity of the optical path. After building up the experimental setup, we increase the pump power, and the PC is slowly adjusted to achieve the mode-locking state. It is found that at a high enough pump power (459 mW or higher), with proper adjustment of the PC, the laser can stably output two types of mode-locked pulses, which are NLP and dissipative soliton, respectively. The NLP mode-locking state can be realized at the pump power of 564 mW, while the dissipative pulses is realized at the pump power of 459 mW. The pulse train is detected by the photodetector (DET08CFC/M) and shown on an oscilloscope (TDS3052B). The pulse width is measured by an autocorrelator (FR-103WS). The spectrum of the pulsed laser is measured by a spectrometer (Q8384). Finally, the radio frequency (RF) spectrum is recorded by an RF spectrum analyzer (N9020A).

3. Experimental results

3.1. NLPs

We first show the experimental results when the laser is operating under the NLP state. At the pump power of 564 mW or even higher, the autocorrelation trace of the NLPs can be obtained, which is characterized by a narrow coherent peak riding a broad pedestal [19]. The pulse train captured by the oscilloscope shows that the pulse repetition rate is 27.43 MHz in figure 2(a). The synchronized dual-wavelength pulses will overlap at the same time position, thus appearing as a single pulse train on the oscilloscope [20]. An RF spectrum around the fundamental repetition rate of 27.43 MHz by using 100 Hz resolution bandwidth (RBW) is described in figure 2(b), showing a SNR of ∼60 dB at the pump power of 1191 mW, which presents a typical characteristic of NLPs. When dual-wavelength synchronous mode-locking is achieved, the pulses of the two wavelengths are strictly synchronized in time, and their repetition rates are exactly the same, thus only one peak is shown in the RF spectrum. By measuring the output pulse width with an autocorrelator and rotating the phase-matching angle of the frequency-doubling crystal ($LiIO_3$), two different NLP widths can be obtained at corresponding different central wavelengths (1055 nm and 1104 nm), which indirectly confirms the generation of dual-wavelength NLP pulses. Furthermore, the pedestal pulse width of the autocorrelation trace is narrower at the shorter wavelength than at the longer wavelength.

The autocorrelation trace of the pulse shown in figure 3 is obtained when the pump power is 1191 mW. We find that there are two phase-matching angle positions of the nonlinear crystal where the autocorrelation traces can be obtained, which means the laser is operating under a dual-wavelength mode-locking state. In addition, by varying the pump power, we measure the pedestal pulse widths and the corresponding spike pulse widths of the two peak wavelengths, as shown in figure 4. Analysis of autocorrelation traces demonstrates an inverse relationship between pedestal durations in the dual-wavelength regime. The 1055 nm spectral band exhibits a 9.82% reduction in the pedestal pulse width (from 31.77 ps to 28.65 ps) as pump power increases from 773 mW to 1191 mW, while the 1104 nm component shows a concomitant 35.62% increase (from 71.71 ps to 97.25 ps) under identical

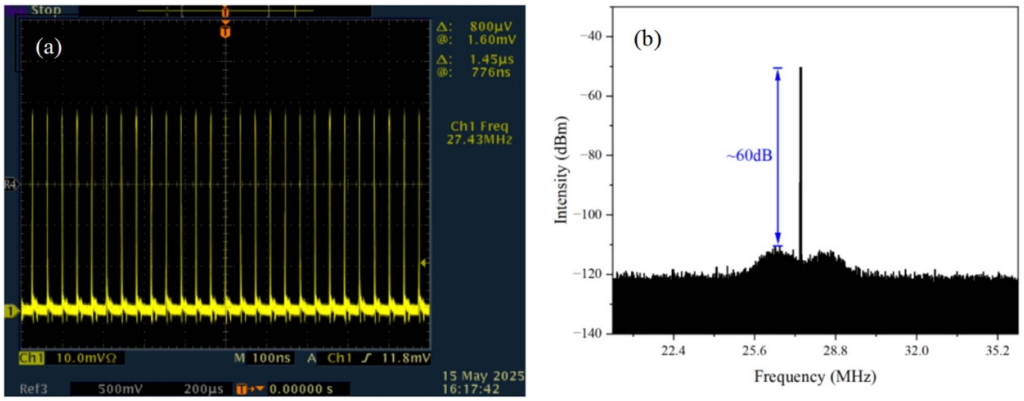

Figure 2. (a) The NLP pulse train shown on an oscilloscope.(b) RF spectrum of the NLP obtained at the pump power of 1191 mW.

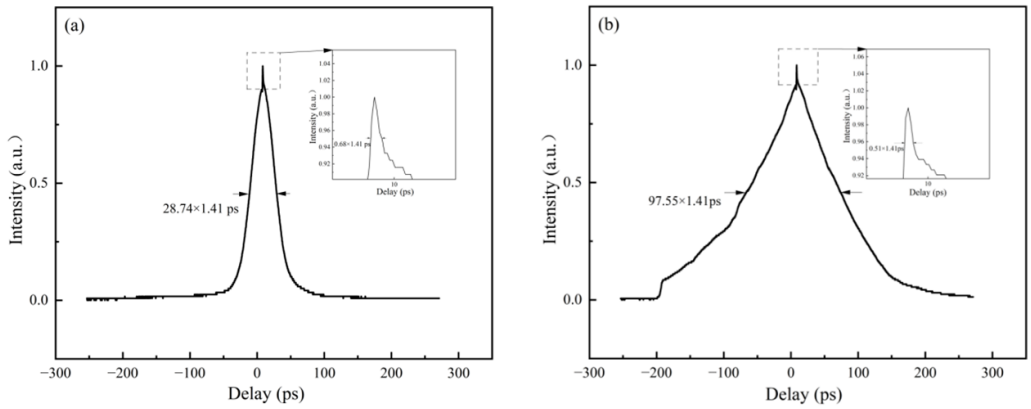

Figure 3. Autocorrelation trace of the NLP obtained at the pump power of 1191 mW: (a) 1055 nm band, and (b) 1104 nm band.

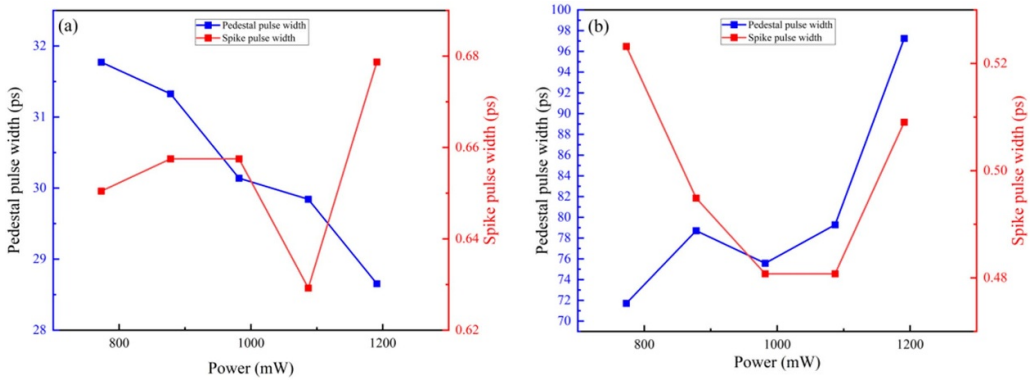

Figure 4. Pedestal pulse widths and corresponding spike widths of NLP at different pump powers: (a) 1055 nm band, and (b) 1104 nm band.

pumping conditions. This counter-proportional behavior suggests competing nonlinear processes between the fundamental and Raman-shifted spectral components, potentially arising from an intracavity energy redistribution. Meanwhile, the spike pulse width of both wavebands does not change too much as the pump power increases.

The relationship between pump power and output power is measured using a power meter, as shown in figure 5(a), the output power increased linearly from 66.3 mW to 140.9 mW with the increase of the pump power from 564 mW to 1191 mW pump power, and the slope efficiency is 12.10%.

As shown in figure 5(b), the spectrum under the NLP state is measured at the pump power of 1191 mW. According to the experimental results, we find that the output spectrum has two peak wavelengths, 1055 nm and 1104 nm. Thus, the laser is under a dual-wavelength mode-locked state. Since 1055 nm is at the emission band of the YDF, it is easy to know that the light in this band is caused by the stimulated radiation of the ytterbium ion. As the pump powers exceeds 564 mW, the nonlinear effect of the fiber is obvious, in which the Raman shift caused by Raman scattering can be expressed as follows: $\Delta k = 1/\lambda_p - 1/\lambda_s$, the wave number of the single-mode silica

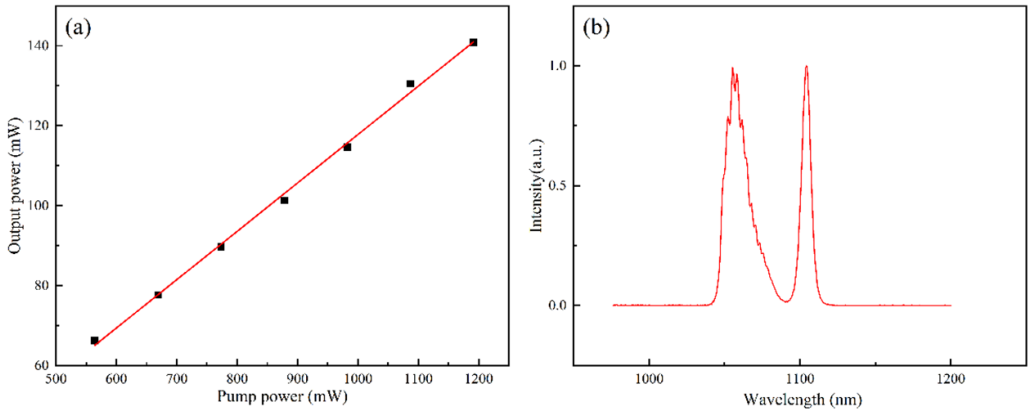

Figure 5. Under the NLP state: (a) output power versus pump power, and (b) the spectrum with the pump power of 1191 mW.

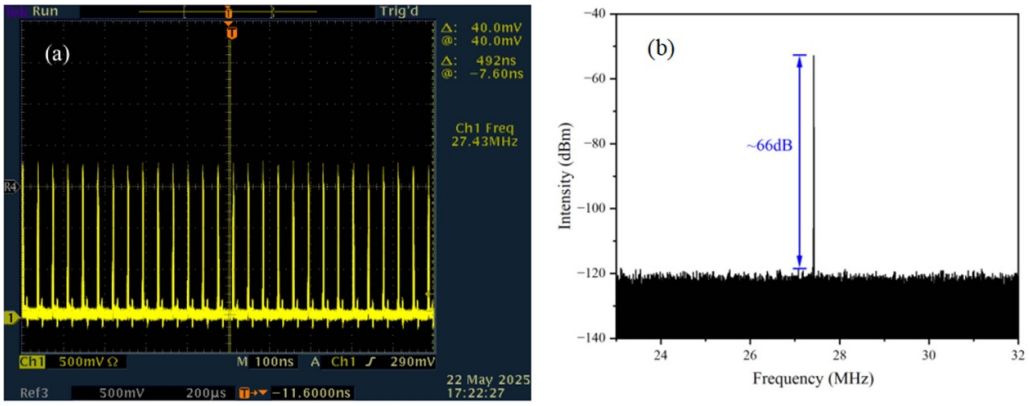

Figure 6. (a) The dissipative pulses train shown on an oscilloscope. (b) RF spectrum of the dissipative pulses obtained at the pump power of 1191 mW.

fiber used in the experiment Δk is 440 cm^{-1} [21], λ_p is the wavelength of the incident photon, and λ_s is the wavelength of the outgoing photon. If $\lambda_p = 1055$ nm, we can find that $\lambda_s = 1105$ nm. Therefore, when the pump power is higher, the light in the 1055 nm band can be regarded as pump for Raman scattering to cause a Raman shift when propagating in the fiber, which generates the light in the 1104 nm band. In summary, we find that the pedestal pulse widths of the two different wave bands (1055 nm and 1104 nm) are around 28.65 ps and 97.25 ps, respectively. Meanwhile, the pulse widths of the spike on the top of the autocorrelation trace are 0.68 ps and 0.51 ps, respectively.

3.2. Dissipative pulses

We then show the experimental results when the laser is operating under the dissipative pulse state. Unlike NLP, dissipative soliton pulses are observed at a pump power of 459 mW. Keeping the structure of the above experimental setup unchanged, the PC is slowly adjusted until the Gaussian-type autocorrelation trace appears on the oscilloscope connected to the autocorrelator. The pulse train captured by the oscilloscope shows that the pulse repetition rate is 27.43 MHz in figure 6(a). The RF spectrum analyzer RBW is 100 Hz, which displays a SNR of 66 dB (when the pump Power is 1191 mW) in figure 6(b).

When the pump power is 1191 mW, the autocorrelation trace of the dissipative pulse is shown in figure 7(a). In addition, by varying the pump power, the pulse width of the dissipative pulse is shown in figure 7(b). In conclusion, the pulse width of the dissipative pulse increases from 20.19 ps to 23.61 ps as the pump power increases from 459 mW to 1191 mW and shows an overall increasing trend. Furthermore, we can only find one autocorrelation trace when we change the phase-matching angle of the crystal in the autocorrelator.

The relationship between pump power and output power is also plotted as shown in figure 8(a), the output power increases with pump power similarly linearly over the 459–1191 mW pump power range, with a slope efficiency of 14.60%.

The spectrum under the dissipative pulse state at the pump power of 1191 mW is shown in figure 8(b), which means that the laser is also working under a dual-wavelength operation state (1044 nm and 1092 nm) due to Raman scattering. During autocorrelation measurements, the phase-matching angles of the frequency-doubling crystal corresponding to the autocorrelation traces of each wavelength are different. When we measured the dissipative pulses, it was found that when the crystal angle is adjusted to the value corresponding to 1044 nm, the autocorrelation trace exhibits dissipative soliton

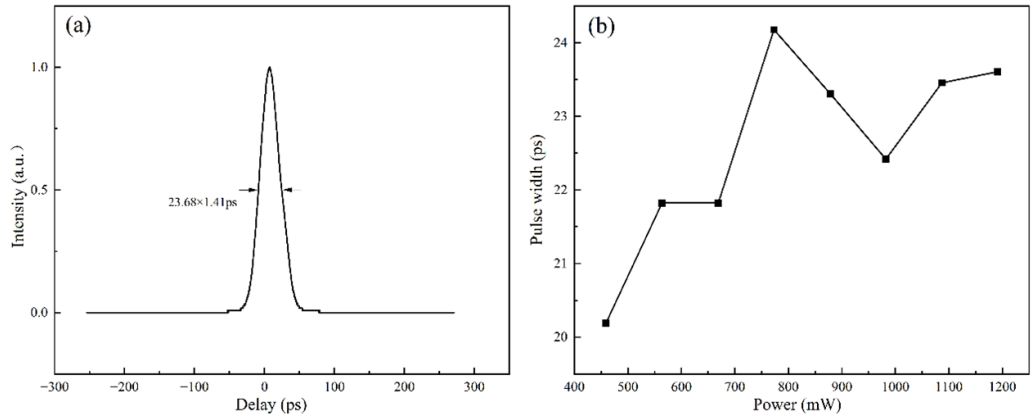

Figure 7. Under the dissipative pulses state: (a) autocorrelation trace obtained at the pump power of 1191 mW, and (b) pulse widths corresponding to different pump powers.

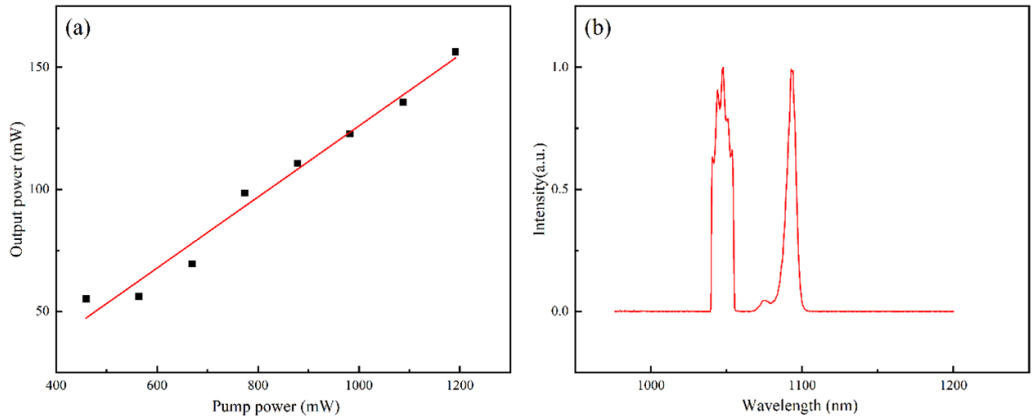

Figure 8. Under the dissipative pulses state: (a) output power versus pump power, and (b) the spectrum with the pump power of 1191 mW.

pulses. However, when the angle of the frequency-doubling crystal is rotated to the value corresponding to the longer wavelength band of 1092 nm, the autocorrelation trace shows no signal. Thus, we find that the laser in the waveband of 1044 nm is working under the mode-locked state, while the laser in the 1092 nm is working under a continuous-wave state.

4. Conclusions

In conclusion, we have experimentally demonstrated a mode-locked dual-wavelength Yb-doped picosecond fiber laser based on NPR. Switching between NLP and dissipative pulse states can be achieved using only a single PC without spectral filters. Compared with the scheme of dual-PC NPR mode-locking, the single PC used in this experiment is placed in front of PD-ISO. This configuration facilitates centralized adjustment of the initial polarization state in the NPR regime. Furthermore, utilizing a single PC not only reduces optical losses but also simplifies the complexity of the optical path. The net dispersion inside the cavity are 0.133 ps^2 (NLP) and 0.129 ps^2 (dissipative soliton) due to different center wavelengths by taking shorter wavelengths (1055 nm and 1044 nm) for example. In general, in NPR mode-locked lasers, nonlinear effects are utilized to make each mode-locked wavelength owns different nonlinear phase shifts, resulting in polarization state differences that enable mode-locking of two wavelengths. Moreover, the central wavelengths of the generated dual-wavelength pulses are relatively close. However, the dual-wavelength pulses generated in this experiment are based on Raman scattering, which is different from the methods used in previous studies. Additionally, the central wavelengths of the generated dual-wavelength pulses are relatively far apart (the peak-to-peak wavelength separation is 49 nm). In an all-normal-dispersion mode-locked fiber laser based on NPR, the mutual switching between NLP and dissipative pulse is achieved by adjusting the intracavity polarization state to alter the positive/negative feedback mechanisms. Negative feedback dominance clamps the peak power to form NLP, while positive feedback dominance enables stable energy amplification to form dissipative pulse [22]. Polarization states play a pivotal role in influencing nonlinear effects and energy distribution. Adjustments to PC can alter the polarization states, subsequently affecting the critical saturation power (CSP) and linear loss ratio (LLR), which in turn influence nonlinear effects and energy distribution. When CSP and LLR undergo changes, the stability of the pulse is disrupted, leading to a transition from dissipative pulse to NLP. During the

transition from dissipative pulse to NLP, this phenomenon can be attributed to nonlinear effects and energy redistribution. NLP pulses exhibit a relatively wider pulse width, whereas dissipative pulse energy is concentrated at the pulse center, resulting in a narrower pulse width [23]. Under the NLP state, the pedestal pulse width in the 1055 nm band shows a decreasing trend (from 31.77 ps to 28.65 ps), while in the 1104 nm band, it increases (from 71.71 ps to 97.25 ps) as the pump power increases. The corresponding output power reaches 140.90 mW, with a slope efficiency of 12.10%. In the dissipative pulse state, the maximum output power increases to 156.40 mW, accompanied by a slope efficiency of 14.60%. The dual-wavelength operation arises from Raman scattering within the fiber cavity, resulting in a Stokes shift in the output spectrum. The pulse width at 1044 nm increases from 20.19 ps to 23.61 ps with increasing pump power. Meanwhile, no autocorrelation trace is observed at the 1092 nm waveband (the Raman peak), indicating that the laser at this wavelength operates in the continuous-wave regime. This implies that only the 1044 nm waveband remains in the mode-locked state. In summary, the laser operates in a dual-wavelength mode-locked state under the NLP regime, with both wavebands mode-locked. However, under the dissipative pulse regime, only the shorter-wavelength component (1044 nm) is mode-locked, while the longer-wavelength component (1092 nm) operates in continuous-wave state. The experimental ring cavity does not contain an extra filter component. Consequently, to achieve stable single-peak wavelength mode-locked pulses, a spectral filter is needed in the experimental setup with reducing the pump power appropriately.

Data availability statement

The data cannot be made publicly available upon publication because no suitable repository exists for hosting data in this field of study. The data that support the findings of this study are available upon reasonable request from the authors.

Conflict of interest

The authors declare no conflicts of interest.

Funding

This study was funded by the National Natural Science Foundation of China (62405017 and 12275017), High-end Foreign Experts Recruitment Plan of China (G2023104003L), Shandong Provincial Natural Science Foundation (ZR2024QF121) and the Ministry of Science and Higher Education of the Russian Federation under Project No. FSWM-2020-0038 and FSUS-2025-0011.

ORCID iDs

Fei He https://orcid.org/0009-0007-1920-618X
Xinyang Su https://orcid.org/0000-0001-8348-0537

References

[1] Keller U 2003 Recent developments in compact ultrafast lasers *Nature* **424** 831–8
[2] Zhu Z, Liu Y, Zhang W, Luo D, Wang C, Zhou L, Deng Z and Li W 2018 Low-noise, robust, all-polarization-maintaining mode-locked Er-doped fiber ring laser *IEEE Photon. Technol. Lett.* **30** 1139–42
[3] Vladimirov A G, Suchkov S, Huyet G and Turitsyn S K 2021 Delay-differential-equation model for mode-locked lasers based on nonlinear optical and amplifying loop mirrors *Phys. Rev. A* **104** 033525
[4] Hao Z, Hu Y, Zhou S, Liu J, Li X, Wang Y and Gao C 2024 Study on spectrum shifting and pulse splitting of mode-locked fiber lasers based on NPR technology *Nanomaterials* **14** 739
[5] Gupta P K, Singh C P, Singh A, Sharma S K, Mukhopadhyay P K and Bindra K S 2016 Chair-like pulses in an all-normal dispersion Ytterbium-doped mode-locked fiber laser *Appl. Opt.* **55** 9961–7
[6] Dong T, Lin J, Zhou Y, Gu C, Yao P and Xu L 2021 Noise-like square pulses in a linear-cavity NPR mode-locked Yb-doped fiber laser *Opt. Laser Technol.* **136** 106740
[7] Geng X, Jiang Y, Gu H, Luo S, Sun M and Li L 2023 A switchable multi-wavelength mode-locked fiber laser based on a multi-mode interference device *Infrared Phys. Technol.* **133** 104812
[8] Pu Y, Guo P, Gao Y, Shen Q, Zhang Z, Fan M and Wang S 2024 Yb-doped mode-locked fiber laser with a hybrid structure of NPR and a Lyot filter as the saturable absorber *Opt. Lett.* **49** 2149–52
[9] Wang Q, Li Z, Xu Q, Sun S, Wang Z, Wang P and Liu Y-G 2024 Nonlinear dynamics of soliton explosion and pulsation in a Yb-doped mode-locked fiber laser *Opt. Fiber Technol.* **88** 103992
[10] Pu Y, Fan M, Shen Q, Guo P, Gao Y and Wang S 2024 Mode-locking and wavelength-tuning of a NPR fiber laser based on optical speckle *Opt. Lett.* **49** 3686–9
[11] Ahmad H, Lutfi M A M, Samion M Z, Zaini M K A and Yusoff N 2024 98 fs high energy stable hybrid mode-locked nonlinear polarization rotation with CuO-doped ZnO saturable absorber *IEEE J. Quantum Electron.* **60** 1300111
[12] Duan J, Yu Q, Qi Y, Jia S, Bai Z, Wang Y and Lu Z 2025 Multipulse bunches in the Yb-doped mode-locked fiber laser based on NLMMI-NPR hybrid mode locked mechanism *Infrared Phys. Technol.* **144** 105646
[13] Su X, Lyu M, Hoang T, Xu Z, Zheng Y and Strickland D 2019 Investigation of long wavelength mid-infrared generation in the tight focusing limit *Opt. Express* **27** 24945–52
[14] Su X, Xu T, Zheng Y and Lü X 2022 Modeling of a dual-wavelength fiber amplification system for further mid-infrared generation *J. Opt.* **24** 065703
[15] Li X *et al* 2023 Passively mode-locked fiber lasers dynamic behavior by multimode fiber polarization controller *Infrared Phys. Technol.* **135** 104989
[16] Li M, Qin L, Li X, Zhang J, Zhang Y, Li J, Li S and Li G 2025 Study on characteristics of noise-like pulses and dissipative soliton resonance pulses in nonlinear multimode interference mode-locked fiber lasers *Opt. Laser Technol.* **187** 112799
[17] Thulasi S and Sivabalan S 2022 Dual wavelength generation and wavelength tunability in Yb-doped mode-locked laser using few-mode fiber as a saturable absorber *Infrared Phys. Technol.* **127** 104409
[18] Tang Y, Li F and Yu X 2022 Dual-wavelength harmonic mode-locked dissipative soliton resonance of Yb fiber laser *Opt. Laser Technol.* **152** 108147

[19] Bravo-Huerta E, Durán-Sánchez M, Álvarez-Tamayo R I, Santiago-Hernández H, Bello-Jiménez M, Posada-Ramírez B, Ibarra-Escamilla B, Pottiez O and Kuzin E A 2019 Single and dual-wavelength noise-like pulses with different shapes in a double-clad Er/Yb fiber laser *Opt. Express* **27** 12349–59

[20] Zhang H, Peng J, Xu G, Zhang Y, Su X, Su Y, Cui M, Zheng Y and Yao J 2024 Observation of operation states and wavelength-switching in spatiotemporal mode-locked lasers *Opt. Laser Technol.* **171** 110462

[21] Stolen R H, Gordon J P, Tomlinson W J and Gordon J P 1989 Raman response function of silica-core fibers *J. Opt. Soc. Am. B* **6** 1159–66

[22] Lang J, Lv C, Lu B and Bai J 2024 Mechanism of noise-like pulse in all-normal dispersion all-fiber laser based on nonlinear polarization rotation *Opt. Express* **32** 2392–404

[23] Kobtsev S, Kukarin S, Smirnov S, Turitsyn S and Latkin A 2009 Generation of double-scale femto/pico-second optical lumps in mode-locked fiber lasers *Opt. Express* **17** 20707–13